

Performance Analysis of Two Low-Noise 0.8 μ m Pixel Designs

Leo Anzagira¹, Jiaju Ma¹, Donald Hondongwa¹, Dexue Zhang¹, Saleh Masoodian¹

¹Gigajot Technology Inc, 3452 E Foothill Blvd, Suite 360, Pasadena, CA 91107

Corresponding Author: leo.anzagira@gigajot.tech

I. INTRODUCTION

Renewed interest in further reducing CMOS image sensor (CIS) pixel sizes and increasing pixel count has led to the development of several sub-micron pixels [1][2][3][4]. Pixel sizes as small as 0.7 μ m have been demonstrated [1] with interest in further decreasing the size to 0.6 μ m. It is well known that continued reduction in pixel size decreases the photodiode capacity, dynamic range (DR) and signal-to-noise ratio (SNR). The Quanta Image sensor (QIS) concept was proposed specifically to address these concerns of reduced storage capacity and dynamic range. QIS addresses these issues by reducing the read noise of the pixels to make them sensitive to single photo-electrons and increasing readout rate so that the pixels require only a small full well capacity (FWC) [5]. Reduced read noise is particularly important to small pixels because of the low signal levels caused by their small area.

II. SENSOR ARCHITECTURE

In this paper, we report the performance of two 0.8 μ m pixel designs in a 2048x256 pixel array manufactured using a commercial 45nm/65nm stacked backside illuminated (BSI) CIS process. The first pixel is based on a standard pinned photodiode (PPD) whilst the second features Gigajot's proprietary pump gate (PG) pixel design [6]. As illustrated in figure 2, the PG pixel uses a distal floating diffusion (FD) design with zero overlap between the transfer gate (TG) and FD whereas the PPD requires some overlap to ensure full charge transfer. Each of the two pixel designs occupies half of the array in the test chip.

A 2x2 shared pixel layout is used for both PPD and PG sub-arrays and the reset (RST), source follower (SF) and row select (RS) transistor designs are identical for both pinned photodiode and the pump gate pixel sub-arrays. Similarly, the rest of the readout architecture is the same for both pixel structures and includes a programmable gain amplifier (PGA), a unity-gain buffer and a 14-bit off-chip ADC. Both pixel structures also have 0.8 μ m-pitch microlenses disposed over a quad Bayer color filter array (CFA) layout. They also employ a 1.6 μ m pitch back deep trench isolation (B-DTI) for crosstalk minimization.

III. CHARACTERIZATION RESULTS

A. Photo Response Performance

The performance of the two 0.8 μ m pixels was evaluated in both light and dark conditions and performance parameters are highlighted in table 1. The light response was characterized with the photon transfer method and transfer curves for the two pixels are shown in figure 3. The two pixels showed good linear light response with less than 0.5% non-linearity and 1.2% photo-response non-uniformity in full resolution mode. The photon-response non-uniformity improves to 0.8% with charge domain binning as the pixel-to-pixel differences within the 2x2 shared group is eliminated. The PPD pixel realizes a full well of 4800e- whilst the PG pixel achieves half of that as a result of differences in optimization of the photodiode implants for the two pixels. Image lag measured using the pulsed light method showed no lag in either pixel design. Both pixels utilize the same optical stack and simulations

show similar internal quantum efficiency (QE), it is therefore expected that measured QE should be similar for the two designs. QE measurements done in the range from 400nm to 1000nm confirmed this expectation. Figure 5 shows the QE curves obtained for the two designs. Very high QE and low spectral color crosstalk was realized considering the pixel size. The blue, red and green pixel QE peaks are located at 450nm, 510nm and 600nm respectively.

A sample color image captured with this sensor is shown in figure 7. The raw image is white balanced and a color correction matrix is applied. The left half of the image which is captured by PG pixel subarray shows no discernible difference from the right half which is made of the PPD subarray.

B. Read Noise and Dark Performance

Dark current was measured at 60C for both pixel designs and hot pixel population compared. Figure 6 shows the dark current distribution for the two sub-arrays. The two designs recorded similar median dark current values with the PPD showing $1.5e^-/\text{sec}/\text{pix}$ compared to $1.4e^-/\text{sec}/\text{pix}$ for the PG pixel. However, from the dark current distribution, the PPD does show a higher population of warm and hot pixels compared to the PG. The population of PPD pixels with dark current greater than $300e^-/\text{pix}/\text{sec}$ is 11ppm compared to 0ppm for the PG. The dark current advantage of the PG pixel may be partly attributed to a larger distance from the photodiode to the silicon surface interface in the pump gate design. In addition to the dark current advantage the PG pixel also demonstrates much better input-referred read noise performance compared to the pinned photodiode. Figure 8 shows the temporal noise distribution for the two pixels measured at room temperature. The PPD design attains a median read noise at $1.35e^-$, which is comparable with previously reported $0.8\mu\text{m}$ pixels using PPDs [2][3], but the pump gate shows a significantly

lower noise level at $0.8e^-$. Since the source follower, reset and row-select transistor designs are identical for both pixel designs, this noise difference between the two pixels is solely due to the pixel design.

IV. CONCLUSION

Overall, both $0.8\mu\text{m}$ pixels show competitive performance compared to the state-of-the art in light and dark performance. The PPD noise and dark current are on par with other $0.8\mu\text{m}$ PPD pixel designs report, however, the PG pixel exceeds the PPD performance and provides distinct advantages that are essential to improving small pixel imaging performance.

V. ACKNOWLEDGEMENTS

The authors appreciate the help provided by TSMC in fabrication of the sensor presented in this work, especially the teams led by F.S. Guo and Y. Yamashita. The authors are also thankful for the advice from E. Fossum, technical discussion with M. Guidash, and technical support from other colleagues at Gigajot Technology.

REFERENCES

1. H. Kim, et al. A $1/2.65\text{in}$ 44Mpixel CMOS Image Sensor with $0.7\mu\text{m}$ Pixels Fabricated in Advanced Full-Depth Deep-Trench Isolation Technology. ISSCC (2020)
2. Park, Donghyuk et al. "A $0.8\mu\text{m}$ Smart Dual Conversion Gain Pixel for 64 Megapixels CMOS Image Sensor with 12k e^- Full-Well Capacitance and Low Dark Noise." 2019 IEEE International Electron Devices Meeting (IEDM) (2019): 16.2.1-16.2.4.
3. T. Hasegawa, et. al. A new $0.8\mu\text{m}$ CMOS image sensor with low RTS noise and high full well capacity. IISW (2019)
4. Okawa, T. et al. "A $1/2\text{inch}$ 48M All PDAF CMOS Image Sensor Using $0.8\mu\text{m}$ Quad Bayer Coding $2\times 2\text{OCL}$ with 1.0lux Minimum AF Illuminance Level." 2019 IEEE International Electron Devices Meeting (IEDM) (2019): 16.3.1-16.3.4.
5. E.R. Fossum, J. Ma, S. Masoodian, L. Anzagira, R. Zizza. The Quanta Image Sensor: Every Photon Counts. *Sensors* (2016),16(8)1260
6. J.Ma, E.R. Fossum, A Pump-Gate Jot Device With High Conversion Gain for a Quanta Image Sensor. JEDS, 2015

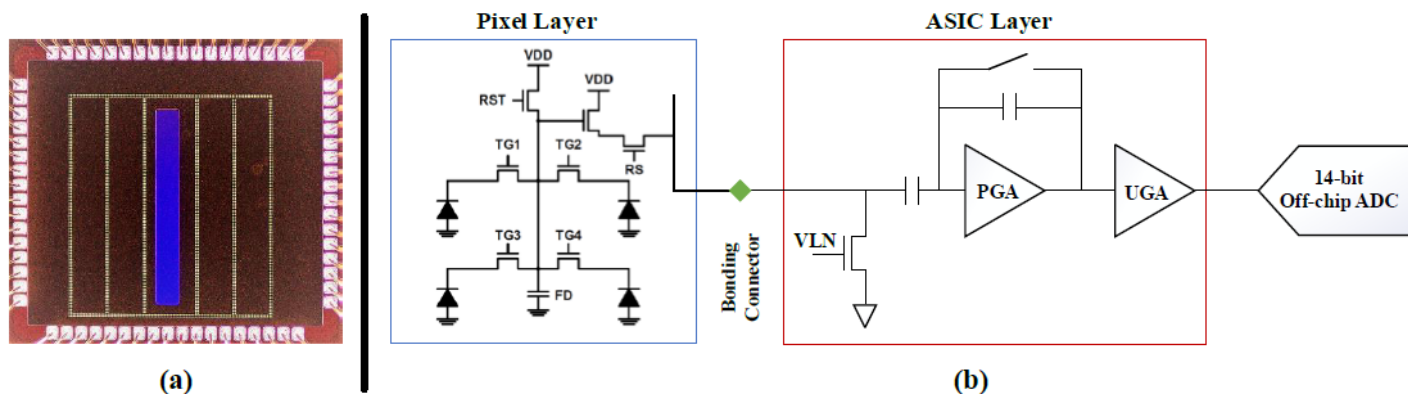


Figure 1. (a) Die Image (b) Sensor architecture showing 2x2 Pixel layout and read out circuitry.

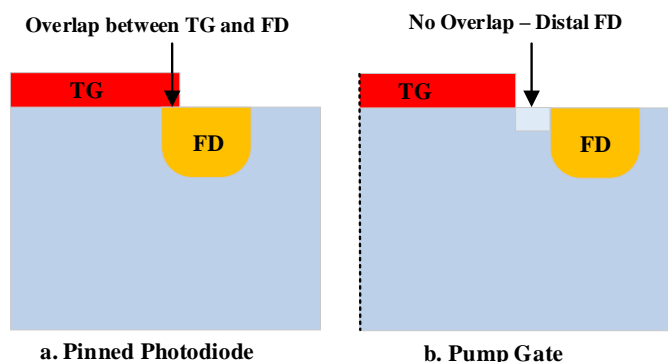


Figure 2: Conceptual Illustration of the fundamental difference between PPDs and Pump Gate Pixels.

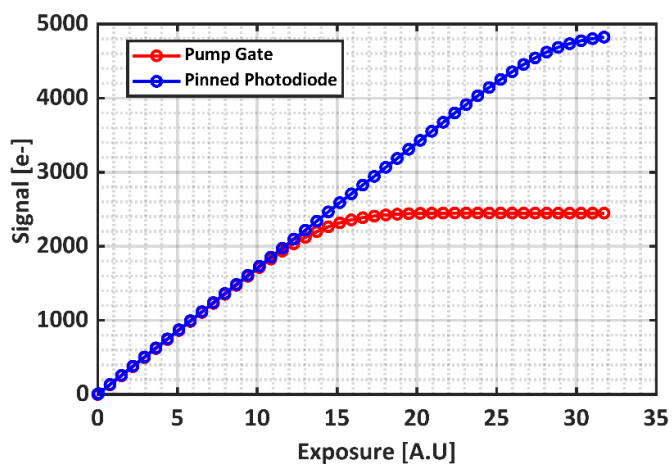


Figure 3: Transfer Curves for PPD and PG pixels. PPD shows a higher full well compared to the PG pixel due to differences in implant optimization.

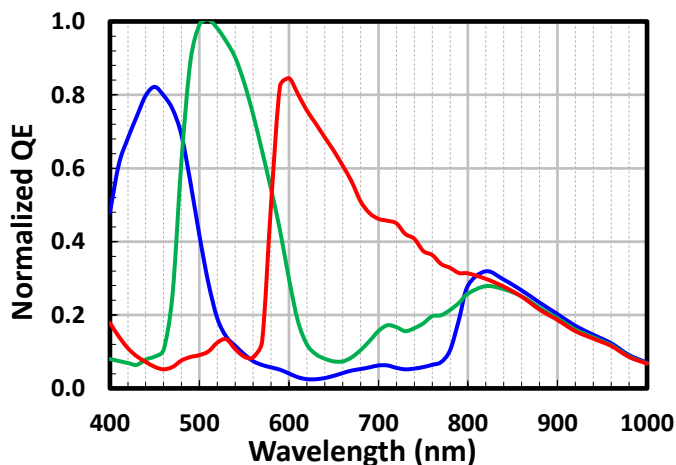


Figure 4: Normalized Quantum efficiency for 0.8um Pixels with Quad Bayer CFA configuration.

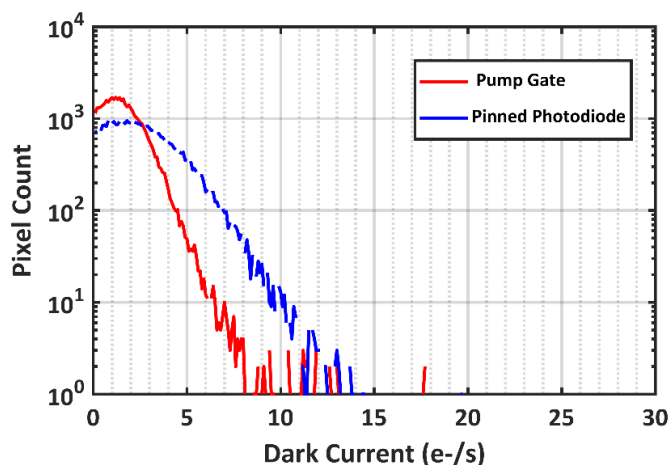


Figure 5: Dark Current measured at 60C. PG pixels shows lower median dark current.



Figure 6: Sample Image captured with sensor. Left half of pixel array contains pump gate pixels and right half is made of PPDs. Full Array size is 256 (V) x 2048 (H).

Table 1: Sensor Performance Summary

		Pump Gate	PPD
Process Technology		45nm/65nm Stacked CIS BSI Process	
Pixel Size		0.8 μ m x 0.8 μ m	
Pixel Resolution		256x2048 (Half PPD and half PG)	
ADC Bit Depth		14 – bit	
Median Pixel Noise		0.8e- rms	1.35e- rms
Full-Well Capacity		2400e-	4800e-
Non-Linearity		<0.5%	<0.5%
PRNU	Full Res	1.2%	1.2%
	Binned	0.8%	0.7%
Median Dark Current @ 60C		1.4e-/pix/sec	1.5e-/pix/sec
Hot Pixels (>300e-/pix/sec)		0 ppm	11 ppm
Lag		<0.2e-	<0.2e-

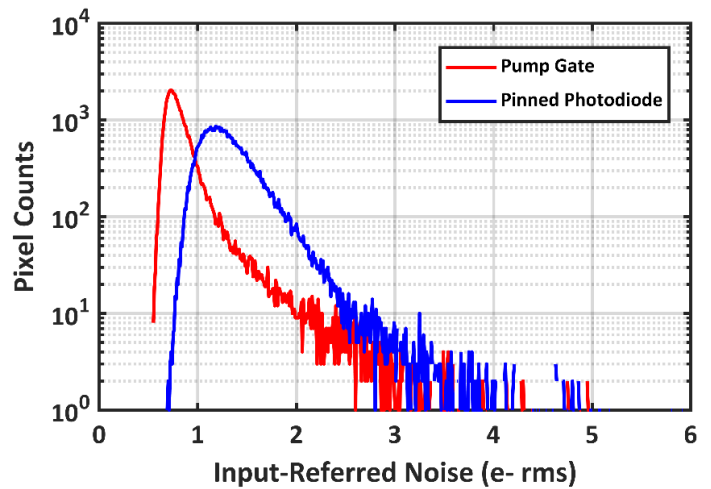


Figure 7: Noise distribution for pinned photodiode and pump gate pixel sub-arrays.